First-principles study of structural and electronic properties of $BaTiO_3(001)$ oxygen-vacancy surfaces

Meng-Qiu Cai,[1,3,*] Yong-Jun Zhang,[2] Zhen Yin,[3] and Ming-Sheng Zhang[3]
[1]*Department of Applied Physics, Hunan University, Changsha, 410082, People's Republic of China*
[2]*Institute of Solid State Physics of JiLin Normal University, SiPing JiLin 136000, People's Republic of China*
[3]*National Laboratory of Solid State Microstructures and Department of Physics, Nanjing University, Nanjing, 210093, People's Republic of China*
(Received 17 December 2004; revised manuscript received 8 June 2005; published 2 August 2005)

The structural and electronic properties of fully-relaxed $BaTiO_3(001)$ surfaces with oxygen vacancies are investigated by first-principles calculations. The large displacements of ions deviated from their crystalline sites to lead to the formation of the surface rumpling have been obtained. Some in-gap Ti 3*d* states at about −1.0 eV below the Fermi level are observed in the Ti-terminated surface caused by the oxygen vacancies. For the Ba-terminated oxygen-vacancy surface, some in-gap Ti 3*d* states also move into the bulk mid-gap region to become partial occupied, and two different chemical states of Ba 5*p* states are found. One is attributed to the bulk perovskite Ba atoms and another one is caused by the relaxation of surface Ba atoms. The calculations are in agreement with experimental data from ultraviolet photoelectron spectroscopy and x-ray photoelectron spectroscopy studies.

DOI: 10.1103/PhysRevB.72.075406 PACS number(s): 68.47.Gh, 77.84.Dy, 73.20.At, 73.20.Hb

I. INTRODUCTION

Barium titanate ($BaTiO_3$) as a typical perovskite ferroelectric material has been intensely investigated for the bulk properties of ferroelectricity, piezoelectricity, and optoelectricity.[1,2] Among these applications, thin films of $BaTiO_3$ are of the greatest interest. However, surface effects in thin film systems have usually great influence on the properties of ferroelectric, optical, and so on.[3,4] It is thus important to investigate the surface properties of $BaTiO_3$ at the near-surface region. The surface properties of $BaTiO_3$ have been widely studied in both experimental and theoretical. In experimental, the electronic properties and ion chemical states of various types of $BaTiO_3$ surfaces have been pursued using ultraviolet-photoemission (UPS) and electron-energy-loss spectroscopy, low-energy electron diffraction (LEED) and Auger spectroscopy.[5–12] The UPS studies showed that there are an enhanced emission at the top of valence and a band gap state at about 0.9 eV below the bottom of the conduction, which reduce by sputtered with Ar ions or O ions but increase when annealed in the oxygen deficient condition (caused oxygen vacancies).[5–8] Note that, the thin film would become conducting due to the presence of the oxygen vacancies, which has been established by photoelectron spectroscopy (PES) studies. The metallic state originates from the electronic states in the bulk band-gap region cause by the Ti 3*d* oxygen vacancy.[7,8] Moreover, for the core-level electronic structure of $BaTiO_3(001)$ vacuum-fractured, two barium core level states were observed using ultraviolet and x-ray photoelectron spectroscopy.[9–12] One was assigned to barium with 12-fold oxygen coordination representative of bulk stoichiometry, and another one assigned to the undercoordinated barium in the region of sample surface. In theoretical, there are some calculations of band structures and electronic states related to the $BaTiO_3$ surface. Marathe *et al.* calculated the $BaTiO_3$ surface using semiempirical molecular orbital (MO) and tight binding approximation method.[13] Cohen presented linearized augmented plane wave calculations performed for slab of tetragonal $BaTiO_3$ with (001) and (111) surface, using both symmetrical and asymmetrical terminations.[14,15] However, atomic positions in the case are not fully relaxed, although some relaxations are allowed. First-principle Hartree-Fock studies of ferroelectric $BaTiO_3$ slab were carried out to analyzed slab polarization and polarization surface charges using the isolated-slab geometry,[16] in which the structure is also unrelaxed. First-principles $BaTiO_3$ electronic structure studies were performed within the periodically repeated slab geometry by the pseudopotential approach with the local density approximation (LDA),[17,18] and an ideal cubic slab was found to possess fully occupied O-2*p* surface states positioned in the M point of the 2D Brillouin zone. Moreover, a first-principles linearized augmented plane wave method studied the mechanism of surface conduction for surface and bulk electronic structures of a free-standing $BaTiO_3$ single slab in vacuum.[19] Recently, Piskunov *et al.* investigated $BaTiO_3(001)$ surface relaxation and electronic structure using the CRYSTAL code based on the *hybrid* (B3PW) exchange-correlation technique.[20] Their data are in good agreement with available calculations and experimental data. However, all the calculations above are based on the perfect $BaTiO_3$ surface. In fact, the oxygen vacancies in the surface of thin film caused by the anneal have great influence on the optical, ferroelectric, and conducting properties of materials.[21] To date, there has not been a comparison between theoretical results and experimental data for the oxygen-vacancy surface and their origin of the surface Ba 5*p* states and in-gap states has not been made clear yet.[5–12]

In this paper, we present a calculation of the fully relativistic slab layer of the $BaTiO_3(001)$ surface in the cubic phase with the oxygen vacancies. Both the symmetrically Ti- and Ba-terminated surfaces are considered, and the atomic configurations have been fully relaxed in our case. Interestingly,

the excellent qualitative and quantitative agreement between experiment and theory gives the substantial evidence of the oxygen vacancies at the surface and surface structural relaxations, which is the reasons for the observed spectral in-gap states and Ba $5p$ surface states of $BaTiO_3(001)$ surfaces.

II. COMPUTATIONAL DETAILS

A. Calculation method

The presented calculations were performed using the full-potential linearized augmented plane-wave method (FLAPW) plus local orbital as embodied in the latest WIEN2K code.[22–24] Integrations in reciprocal space were performed by using the tetrahedrons method with a k mesh of 15 k points in the two-dimensional irreducible Brillouin zone. In the FLAPW method the relevant convergence parameter is $R_{mt}K_{\max}$ defined by the product of the smallest atomic sphere radius (R_{mt}) times the largest reciprocal lattice vector of the plane-wave basis ($K_{\max}$). For controlling the size of the basis set for the wave functions, the parameter $R_{mt}K_{\max}$ was set to 6.0 and make the expansion up to $l=12$ in the muffin tins, containing a well-converged basis set of about 1800 LAPW's. Convergence tests indicate that only small changes result from going to a denser k mesh or to a larger value of $R_{mt}K_{\max}$. The self-consistent calculations are considered to be converged only when the integrated charge difference performula unit $\int|\rho_n-\rho_{n-1}|dr$ between input charge density $[\rho_{n-1}]$ and output $[\rho_n]$ is less than 0.0001.

B. Surface models

We modeled the surface by a periodic slab of nine layers with TiO_2 and BaO stacked alternately, separated by a vacuum of the same thickness as the slab. Two kinds of slabs with the Ti-terminated (slab I) and and Ba-terminated (slab II) surface are considered (A schematic diagram of these two configurations can be found in Ref. 17). The z axis is taken as orthogonal to the surface, and the M_z mirror symmetry with respect to the central layer was imposed in all cases. These slabs are finite in the z direction but periodic in the x and y directions. Oxygen vacancy is introduced as a defect by removing a surface oxygen atom. As a comparison, the perfect surface are also investigated in this paper. The schematic illustrations viewed from the top of the slabs for the Ba- and Ti-terminated surfaces are shown in Fig. 1. In our calculations, we adopted experimental lattice constants a_c 7.554 a.u. for the bulk $BaTiO_3$.

III. RESULTS AND DISCUSSION

A. Slab and vacuum thickness

For the periodically repeated artificial slab geometry, two surfaces would strongly interact both via the "bulk" as well as via "vacuum" on condition that there are few slab layers or reduced vacuum. The spurious interactions leads to a splitting of the two surface states.[25,26] On the other hand, even moderate vacuum separations and slab thickness greatly increase the computational burden. In order to select the right size of the slab and vacuum thickness, we have calculated the working function[19] (WF) of the slabs and the electric field gradient (EFG) of the surface atoms.[27,28] In general, the EFG of the surface atom should converge for slab thickness upon a thick enough vacuum thickness and the WF should convergence for the vacuum thickness upon a thick enough slab thickness. The working function (WF) is defined as follows: $\mathrm{WF}=V_c-E_F$, where V_c is the Coulomb potential at the center of the vacuum and E_F presents the Fermi-energy of the slab. The calculations show that, when the value of the slab and vacuum thickness are all equal to 30.216 a.u., the value of the EFG and WF is good convergent. Therefore, we adopt the value of 30.216 a.u. for both the slab and vacuum thickness in our calculations.

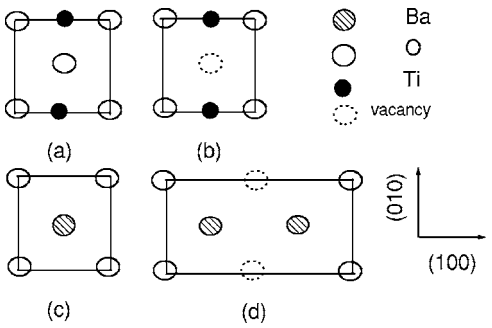

FIG. 1. The top view of two possible terminations (Ti-terminated slab I and Ba-terminated slab II) for the $BaTiO_3$ (001) surfaces: (a) 1×1 cell for perfect surface with Ti termination (slab I), (b) 1×1 cell for oxygen-vacancy surface with Ti termination (slab I), (c) 1×1 cell for perfect surface with Ba termination (slab II), (d) 2×1 cell for oxygen-vacancy surface with Ba termination (slab II).

B. Structural relaxation

First, equilibrium positions of atoms were evaluated by a damped Newtom dynamics method by calculating the Hellman-Feynman forces,[29] and the final forces on each atoms was less than 1 mRy/a.u.. We start from the ideal structure and relaxed atomic positions in the slab are measured with respect to the corresponding undistorted bulk $BaTiO_3$. The relaxed geometries of Ti and Ba termination in the z direction are summarized in Table I and II, respectively. The displacements are only listed for the atoms in the top half of the slabs, and others are determined by the mirror symmetry. The positive displacements in the [001] direction denote the relaxations toward the vacuum region, and the magnitudes, given as fraction of cubic lattice constant a_c, are measured with respect to ideal positions.

From Table I, we can see that the largest relaxations are on the surface-layer atoms for the perfect and the defect surface of the Ti-terminated slabs. For the perfect surface, relaxation includes a displacement of Ti atoms by $-0.0264a_c$ and a displacement of the O atoms by $+0.0026a_c$ at the surface layer. At the subsurface layer, relaxation includes a displacement of Ba atoms by $+0.0259a_c$, and a displacement of O atoms by $-0.0046a_c$. Consequently, the surface dipole

TABLE I. Atomic relaxations of the Ti-terminated surface (slab I) in the cubic phase. The positive (negative) displacements in the [001] direction denote the atomic displacements outwards (inwards) the vacuum region and the magnitudes, given as a fraction of cubic lattice constant a_c, are measured with respect to ideal positions.

	perfect surface			
Atom	FLAPW-HL[a]	UPA-LDA[b]	FLAPW-GGA[c]	defect surface FLAPW-GGA[d]
Ti (1)	−0.0210	−0.0389	−0.0264	−0.0113
O (1)	0.0070	−0.0163	0.0026	0.0464
Ba (2)	0.0220	0.0131	0.0259	−0.0026
O (2)	−0.0090	−0.0062	0.0046	0.0422
Ti (3)		−0.0075	−0.0044	−0.0192
O (3)		−0.0035	0.0002	0.0127
Ba (4)			0.0042	−0.0047
O (4)			0.0011	0.0006

[a]Ref. 19 (perfect surface with nine layer slabs).
[b]Ref. 17 [perfect surface with seven layer slabs with the ultrasoft-pseudopotential approach (UPA)].
[c]Present work for the perfect surface with nine layer slabs.
[d]Present work for the oxygen vacancy surface with nine layer slabs.

points away from, whereas the subsurface dipole points toward the vacuum regions. The layer-by-layer dipole rapidly decrease in the magnitude from surface layer toward the inner. Thus, the slab is paraelectric with zero net polarization. This relaxation pattern (i.e., the buckling of the surface layer, together with the decrease of the first interlayer spacing) is in qualitative agreement with the finding of Ref. 19. The relaxation of the third plane is already quite small. Moreover, the relaxed direction of the metal atoms and oxygen atoms is different leading rumpling of the surface layers. The atomic displacements in the outmost two layers are good agreement with the full-potential linearized augmented plane-wave method with Hedin-Lundquist exchange-correlation potential (FLAPW-HL) calculations[19] but rather than the ultrasoft-pseudopotential approach with local density approximation (UPA-LDA) calculations,[17] especially for the surface-layer atoms. In our calculations, for the oxygen vacancy slab, the direction and the magnitudes of the atomic displacements are quite different from those of the perfect slab due to the oxygen vacancies at the surface layer. The surface Ti ions shift inwards by $0.0113a_c$, which is smaller than that of the perfect surface, and the surface oxygen ions shift outwards $0.0464a_c$, which is larger than that of the perfect surface. At the subsurface layer, the displacements of Ba and O ions are inward $0.0026a_c$ and outward $0.0422a_c$, respectively, which are the opposite sign with respect to those of the Ba and the O ions in the subsurface layer of the perfect slab. At the surface layer, owing to the larger relaxations of the Ti and O ions in the opposite directions, it would lead to larger rumpling than that of the perfect surface.

As for the Ba-terminated surface, the largest relaxations are on the subsurface-layer atoms not on the surface-layer atoms. Because of the ionic state of the Ba, the influence on the relaxation in the Ti—O layer is larger than in the Ba—O layer. Compared to the results by ultrasoft-pseudopotential approach (UPA),[17] there are some difference about the surface structural relaxations for the direction and the magnitudes of the slab atoms. However, there have not been any experimental surface structural relaxation and rumpling determination for $BaTiO_3$. Thus, our calculations could be interested in more detailed experiments on the surface rumpling and relaxation.

TABLE II. Atomic relaxations of the Ba—O-terminated surface (slab II) in the cubic phase. The positive (negative) displacements in the [001] direction denote the atomic displacements outwards (inwards) the vacuum region and the magnitudes, given as a fraction of cubic lattice constant a_c, are measured with respect to ideal positions.

	perfect surface		
Atom	UPA-LDA[a]	FLAPW-GGA[b]	oxygen vacancy surface FLAPW-GGA[c]
Ba (1)	−0.0279	−0.0104	−0.0006
O (1)	−0.0140	0.0033	0.0018
Ti (2)	0.0092	0.0222	0.0037
O (2)	0.0048	0.0171	0.0071
Ba (3)	−0.0053	−0.0014	−0.0002
O (3)	−0.0026	0.0040	0.0031
Ti (4)		0.0041	0.0008
O (4)		0.0003	0.0013

[a]Ref. 17 [perfect surface with seven layer slabs with the ultrasoft-pseudopotential approach (UPA)).
[b]Present work for the perfect surface with nine layer slabs.
[c]Present work for the oxygen vacancy surface with nine layer slabs.

C. Surface electronic band structure

Figures 2(a)–2(c) show the calculated band structure projected onto the surface Brilluoin zone for the bulk $BaTiO_3$, the perfect $BaTiO_3(001)$ surface by Ti-terminated, and the oxygen-vacancy $BaTiO_3(001)$ Ti-terminated surface, respectively. For the perfect face, the band gap is reduced, and there is a tendency for valance-band states to intrude upwards into the lower part of the band gap, especially near the M point of surface BZ.[17,19] The surface states consists of the pair of states due to the surface oxygen atom. The states are positioned within the lower part of the bulk band gap. They are nearly degenerate, fully occupied, and uncharged. For the the perfect $BaTiO_3(001)$ Ti-terminated surface, no deep gap states appear in spite of the present of effective surface potential due to the imperfect ligand configuration at the top layer [Fig. 2(b)]. As compared to the projected bulk band [Fig. 2(a)], the band structure for the perfect surface has a semiconducting feature. The tops of the valence band near the Γ and M points show a remarkable change, i.e., the top of the valence bands with the smaller effective mass shifts to the high-energy positions as compared with the top of the heavier bands. The top parts of the valence bands with the lighter mass are considered to form the surface states. Surface effects mostly appear in the valence band rather than the

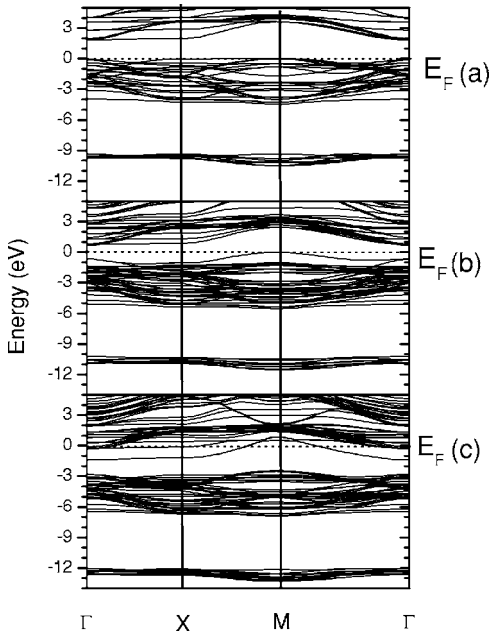

FIG. 2. Energy band structure for $BaTiO_3$ in the cubic phase. (a) Bulk band structure projected to surface. (b) Band structure of perfect $BaTiO_3$ (001) surface with Ti termination (slab I). (c) Band structure of oxygen-vacancy $BaTiO_3$ (001) surface with Ti termination (slab I). The zero of energy corresponds to the bulk valence maximum and only the lowest few conduction bands are shown.

conduction bands. However, as shown in Fig. 2(c), the electronic band structure of the oxygen-vacancy surface is quite different from those of bulk and perfect surface. There are two significant groups of states associated with the Ti-terminated surface with oxygen vacancies. First, some states in the conduction band are remarkably lowered and pulled down in the band-gap region and they go across the Fermi level. Since the conduction bands are predominantly formed by the Ti 3*d* components, the partial occupation of the band is due to the electron transfer into some of Ti 3*d* orbitals. It is necessarily associated with the oxygen vacancies: electrons enter the Ti 3*d* band due to the lack of O 2*p* states. As seen from the band structure in Fig. 2(c), the surface becomes metallic. The feature of the metallic surfaces has been known from the experimental studies, which was ascribed to electronic state at the spatially ordered Ti 3*d*-oxygen vacancies on the surface.[7,8] In contrast to the band structure of the perfect surface [Fig. 2(b)], the surface states in the valence band are suppressed and the surface states at the *M* point of the oxygen-vacancy surface are less obvious than those of the perfect surface.

Figures 3(a)–3(c) show the total density of states of the bulk with cubic $BaTiO_3$, the perfect surface $BaTiO_3(001)$ with Ti-termination, and the oxygen-vacancy $BaTiO_3(001)$ surface with Ti termination. It is clearly that, as the relaxations of atoms, the optical gap is reduced from 1.87 eV for the bulk down to about 0.8 eV for the perfect surface with Ti termination. For the perfect surface, some surface states caused by the relaxations of the surface oxygen atoms for the A point, shown in Figs. 3(b), toward to the bulk gap, and the surface is insulated. But for the oxygen-vacancy $BaTiO_3(001)$ surface with the Ti termination, there are some

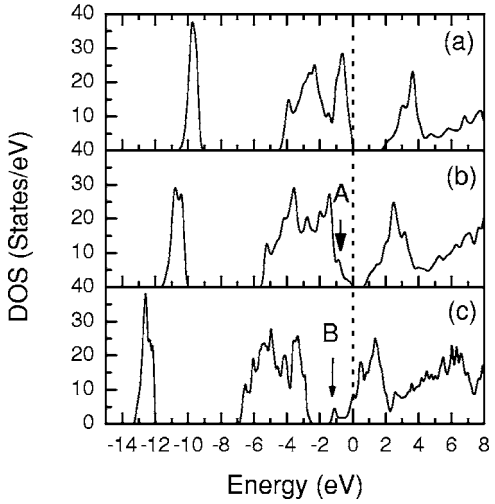

FIG. 3. Total density of states (DOS) for $BaTiO_3$. (a) bulk DOS. (b) DOS for perfect 1×1 cell surface with Ti termination (slab I). (c) DOS for defect 1×1 cell surface with Ti termination (slab I). Peak A is the surface states of O 2*p* for the perfect surface and peak B is the in-gap states of Ti 3*d* for the defect surface.

in-gap states introduced in the region of the bulk gap. A sharp peak is positioned at about −1.0 eV below the Fermi level, which is excellent agreement with the experimental results by UPS.[5–8] Because of the conduction of the oxygen-vacancy surface, the larger leakage current for the thin film with some oxygen vacancies than that of the bulk.

In order to clarify the in-gap states of the oxygen-vacancy surface with the Ti termination, we plot the partial density of states of the Ti 3*d* orbital in the different slab layer. The 3*d* states of the Ti atoms in the surface layer, the third layer, and the center layer are shown in Figs. 4(a)–4(c), respectively. Compared to the total density of states [Fig. 3(c)], the in-gap states for the *B* point, clearly, attribute to the surface Ti atoms, which are introduced by the oxygen vacancies in the surface layer. Because of the loss of the O 2*p* states, some

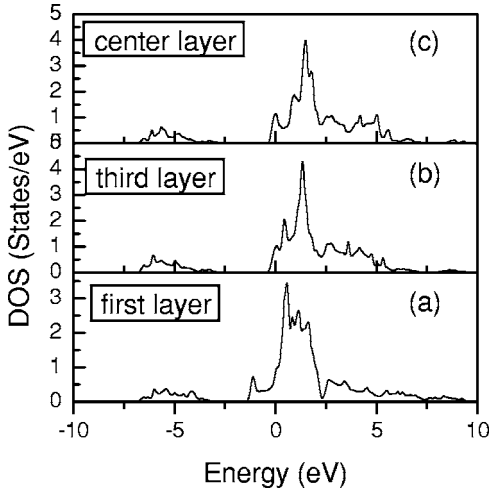

FIG. 4. The projected partial density of states (DOS) of Ti 3*d* states for the defect surface with Ti termination (slab I) in (a) the surface layer, (b) the third layer, and (c) the center (bulk) layer, respectively.

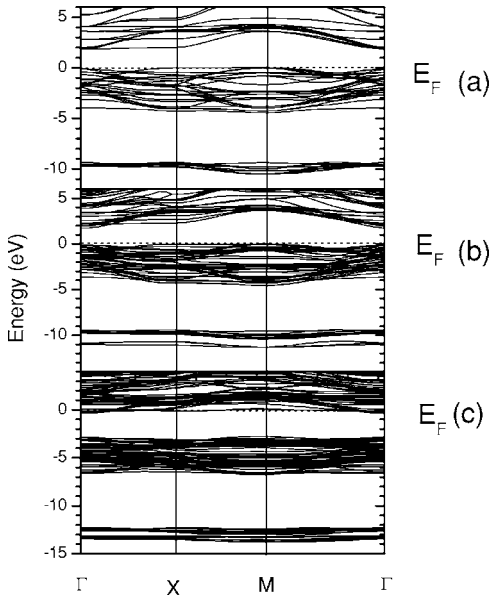

FIG. 5. Energy band structure of $BaTiO_3$ for (a) bulk, (b) perfect 1×1 cell surface with Ba termination (slab II), (c) defect 2×1 cell surface with Ba termination (slab II).

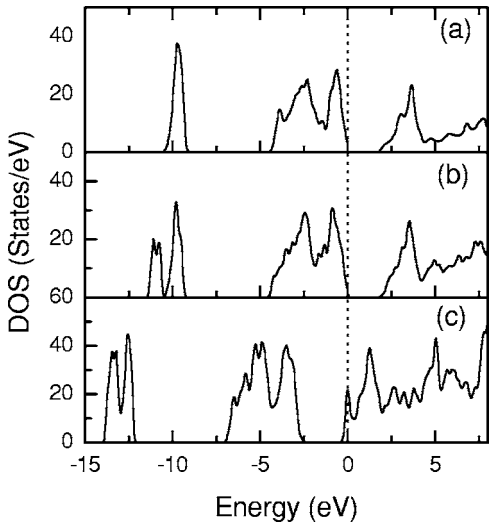

FIG. 6. Calculated total density of states (DOS) of $BaTiO_3$ in the cubic phase. (a) bulk DOS. (b) DOS for perfect surface with Ba termination (slab II). (c) DOS for defect surface with Ba termination (slab II).

electrons move into the Ti 3*d* orbital, and then the Ti 3*d* become partially occupied and metallic. Definitely, due to the charge transferring, the *d* orbital of Ti atoms in the third layer and the center layer also become occupied and low conduction. Note that large effects are mainly caused by the surface Ti atoms.

In the following part, we should discuss the electronic band structure for the perfect and oxygen-vacancy $BaTiO_3(001)$ surface with Ba-termination. Although there are several experimental papers for the surface chemistry of Ba^{2-} ion,[9–12] there have not been any theoretical works for this issue. Figures 5(a)–5(c) show the electronic band structure of bulk, perfect, and oxygen-vacancy $BaTiO_3(001)$ surface with Ba termination, respectively. Compared with the bulk electronic structure, the electronic band structure of the perfect and oxygen-vacancy $BaTiO_3(001)$ slab with Ba termination have obviously difference. For the perfect surface, we can see that the valence band O 2*p* states and the conduction band Ti 3*d* states have few difference from the bulk band structure. Moreover, the band gap for the perfect surface with Ba-terminated slab does not change much with respect to its bulk case, and no in-gap state occurs. All of these are consistent with previous reports.[17] However, our calculated results show that there are two different chemical states for the Ba 5*p* states. One is positioned at about −10.0 eV below the Fermi-level, and another one is positioned at about −11.0 eV. As for the oxygen-vacancy surface, note that a definite difference from the perfect surface is that some conduction band Ti 3*d* states cross the Fermi surface and become partially occupied, which is caused by the loss of oxygen atoms. Therefore, the surface become metallic. In the same case, there are also two chemical states for the Ba 5*p* states, and the surface states for the the valence band O 2*p* states are suppressed. In order to explicitly compare the different electronic structure of bulk, perfect and oxygen-vacancy surface, we plot the total density of states for the three cases shown in Figs. 6(a)–6(c), respectively. For the valence band, except that the O 2*p* and Ba 5*p* states shift toward low energy for the oxygen-vacancy surface, there is little difference for the electronic structure of the valence band between perfect surface and oxygen-vacancy surface. However, some Ti 3*d* conduction band are introduced into the bulk band gap and become partially occupied for the oxygen-vacancy surface. By exploring the partial density of states of Ba atoms in the center bulk layer and surface layer for the perfect and oxygen-vacancy $BaTiO_3(001)$ slab with Ba termination, We think that the two different chemical states in the low- and high-energy region for the perfect and oxygen-vacancy surface are caused by the relaxation of surface Ba atoms and center Ba atoms, respectively. Importantly, our calculations for the surface chemical states of Ba atoms are in good agreement with the x-ray photoelectron spectroscopy.[9–12]

IV. CONCLUSION

In summary, we have calculated the structural and electronic properties of $BaTiO_3(001)$ surfaces in the cubic phase with oxygen vacancies by using first-principles FLAPW method. Both the symmetrically Ti- and Ba-terminated surfaces are considered, and the atomic configurations have been fully relaxed. For the Ti-terminated defect surface, some in-gap titanium 3*d* states at about 1.0 eV below the Fermi level are observed, and the surface becomes metallic. For the Ba-terminated defect surface, some titanium 3*d* states move into the bulk midgap to become partial occupied and conducting, and the surface states Ba 5*p* are caused by the relaxation of the surface Ba atoms.

ACKNOWLEDGMENTS

This work has been supported by the National Natural Science Foundation of China through Grant Nos. 10174034

and 10374047 and the Natural Science Foundation of Jiangsu Province through Grant No. BK2001026. The authors would express their thanks to the Supercomputer Center of Nanjing University for computation support. The calculation was performed at computer SGI Origin 3800 using the WIEN2K code.

---

*Electronic address: caimengqiu@nju.org.cn

[1] M. Q. Cai, Z. Yin, and M. S. Zhang, Appl. Phys. Lett. **83**, 2805 (2003).
[2] R. E. Cohen, Nature (London) **358**, 136 (1992).
[3] J. Junquera and P. Ghosez, Nature (London) **422**, 506 (2003).
[4] B. Meyer and D. Vanderbilt, Phys. Rev. B **63**, 205426 (2001).
[5] T. Shimizo, H. Bando, Y. Aiura, and Y. Haruyama, Jpn. J. Appl. Phys., Part 2 **34**, L1305 (1995).
[6] H. Bando, T. Shimitzu, Y. Haruyama, K. Oka, and Y. Nishihara, J. Vac. Sci. Technol. B **14**, 1060 (1996).
[7] R. Courths, Phys. Status Solidi B **100**, 135 (1980).
[8] S. W. Robey, L. T. Hudson, V. E. Henrich, C. Eylem, and B. Eichhorn, J. Phys. Chem. Solids **57**, 1385 (1996).
[9] L. T. Hudson, R. L. Kurtz, S. W. Robey, D. Temple, and R. L. Stockbauer, Phys. Rev. B **47**, 10832 (1993).
[10] L. T. Hudson, R. L. Kurtz, and S. W. Robey, D. Temple, and R. L. Stockbauer, Phys. Rev. B **47**, 1174 (1993).
[11] B. Cord and R. Courths, Surf. Sci. **152**, 1141 (1985).
[12] M. S. Mukhopadhyay and T. C. S. Chen, J. Mater. Res. **10**, 1052 (1995).
[13] V. R. Marathe, S. Lauer, and A. Trautwein, Phys. Status Solidi B **100**, 149 (1980).
[14] R. E. Cohen, J. Phys. Chem. Solids **57**, 1393 (1996).
[15] R. E. Cohen, Ferroelectrics **194**, 323 (1997).
[16] L. Fu, E. Yaschenko, L. Resca, and R. Resta, Phys. Rev. B **60**, 2697 (1999).
[17] J. Padilla and D. Vanderbilt, Phys. Rev. B **56**, 1625 (1997).
[18] X. Y. Xue, C. L. Wang, and W. L. Zhong, Surf. Sci. **550**, 73 (2004).
[19] M. Krčmar and C. L. Fu, Phys. Rev. B **68**, 115404 (2003).
[20] S. Piskunov, E. A. Kotomin, E. Heifets, J. Maier, R. I. Eglitis, and G. Borstel, Surf. Sci. **575**, 75 (2005).
[21] R. I. Eglitis, N. E. Christensen, E. A. Kotomin, A. V. Postnikov, and G. Borstel, Phys. Rev. B **56**, 8599 (2003).
[22] D. J. Singh, *Planewaves, Pseudopotentials and LAPW Method* (Kluwer Academic, Boston, 1994).
[23] P. Blaha, K. Schwarz, G. K. H. Madsen, D. Kvasnicka, and J. Luitz, *WIEN2K* (Technical University of Vienna, Austria, 2001).
[24] J. P. Perdew, K. Burke, and M. Ernzerhof, Phys. Rev. Lett. **77**, 3865 (1996).
[25] N. Takeuchi, C. T. Chan, and K. M. Ho, Phys. Rev. B **43**, 13899 (1991).
[26] G. Nicolay, F. Reinert, S. Hüfner, and P. Blaha, Phys. Rev. B **65**, 033407 (2001).
[27] L. A. Errico, G. Fabricius, M. Renteria, P. delaPresa, and M. Forker, Phys. Rev. Lett. **89**, 055503 (2002).
[28] R. Laskowski, G. K. H. Madsen, P. Blaha, and K. Schwarz, Phys. Rev. B **69**, 140408(R) (2004).
[29] R. Yu, D. Singh, and H. Krakauer, Phys. Rev. B **43**, 6411 (1991).